

Functional silver coated colloidosomes as targeted carriers for small molecules

*Qian Sun*¹, *Yao Du*¹, *Ziyan Zhao*¹, *Elizabeth A. H. Hall*¹, *Hui Gao*², *Gleb B. Sukhorukov*²,
Alexander F. Routh^{1*}

AUTHOR ADDRESS

1- Department of Chemical Engineering and Biotechnology, University of Cambridge, Pembroke Street, CB2 3RA, Cambridge, United Kingdom

2- School of Engineering and Materials Science, Queen Mary University of London, Mile End Road, E1 4NS, London, United Kingdom

ABSTRACT

Colloidosomes have attracted great interest in recent years because of their capability for storage and delivery of small molecules for medical and pharmaceutical applications. However, traditional polymer shell colloidosomes leak low molecular weight drugs due to their intrinsic shell permeability. Here, we report aqueous core colloidosomes with a silver shell, which seals the core and makes the shell impermeable. The silver coated colloidosomes were prepared by reacting L-Ascorbic acid in the microcapsule core with silver nitrate in the wash solution. The silver shell colloidosomes were then modified by using 4,4'-dithiodibutyric acid and crosslinked with rabbit Immunoglobulin G (IgG). Label-free Surface Plasmon Resonance was used to test the specific targeting of the functional silver shell with rabbit antigen. To break the shells, ultrasound treatment was used. The results demonstrate that a new type of functional silver coated colloidosome with immunoassay targeting, non-permeability, and ultrasound sensitivity could be applied to many medical applications.

INTRODUCTION

Small hydrophilic drug molecules are widely used in the pharmaceutical industry and play an important role in medical applications. However, their characteristics including rapid clearance, suboptimal biodistribution, toxicity, nonspecific targeting as well as low intracellular absorption can limit their therapeutic efficacy^[1-4]. An approach to avoid these limitations is to encapsulate the drugs in carriers, which can deliver them to targeted areas, before releasing them to achieve their functions^[5]. During the past 20 years, water core colloidosomes have attracted great interest, since they have a good capability to load and deliver small molecules^[6-10]. For example, they can be used to delay the release of an active drug species, until the reaction conditions are suitable^[11]. In medical applications, colloidosomes can be used as drug delivery systems with targeted delivery and controlled release options^[12-14].

Most polymer shell colloidosomes are leaky to small molecules due to the intrinsic permeability of their shells. This greatly limits their practical application in medical fields^[15-19]. In a previous study, we synthesized impermeable silver coated colloidosomes achieved by using L-Ascorbic acid in the core and silver nitrate (AgNO_3) in the wash solution^[20]. The shell was chosen because silver particles are widely used in biomedical applications^[21-23], especially for thiol linkers to selectively bind receptor proteins in targeted drug delivery applications^[24-26].

As well as encapsulation, the suppression of non-specific targeting also needs to be solved. When using capsules for controlled drug delivery, it may be necessary to target the drug to particular places or cells in the body and to control the duration of action of the drug^[27]. In this paper we used thiol chemistry to modify the colloidosomes and to crosslink the impermeable modified silver shell colloidosomes with rabbit Immunoglobulin G (IgG), as a model to demonstrate specific targeting. The silver shell colloidosomes may quench any

fluorescence or dye tagging signal ^[28-31], which could affect fluorescence. To solve this problem, a Surface Plasmon Resonance (SPR) biosensor was used to test if the colloidosomes are specifically attached to a surface modified with anti-rabbit IgG ^[32-35]. The SPR biosensor is a label-free and high-sensitivity technique, which has been widely used for quantitative analysis of various target biomolecules ^[36, 37]. In addition, we examined the permeability of the silver coated colloidosomes to dye solution (Allura Red AC) and demonstrate breakage of the silver shell using an ultrasound treatment.

Unlike many drug carriers, the functional silver coated colloidosomes have the capability of specific targeting as well as small molecule encapsulation and their release can be triggered by ultrasound. For example, compared with the impermeable silver shells, most traditional polymer shell capsules will leak small molecule materials after a few hours ^[6-10, 15-19]. In addition, manufacture of colloidosomes in this way avoids the use of high temperatures and high concentrations of harsh solvents. For instance, the making process of some MOFs metal vesicles ^[38, 39] and metal shells ^[40] need to use solvent or high temperatures. Hence, the silver coated colloidosomes are ideal to meet the demands of medical applications, which include targeted carriers for small molecules and controlled drug delivery.

EXPERIMENTAL SECTION

Materials. The water used in all experiments was deionized of resistivity 18.2 M Ω •cm produced by a Pure Lab Ultra apparatus. Sodium dodecyl sulfate (SDS, Fisher Scientific), Allura Red AC dye (Sigma-Aldrich), 4,4'-dithiodibutyric acid (DDA, 95%, Sigma-Aldrich), N-hydroxysulfosuccinimide sodium salt (Sulfo-NHS, \geq 98%, Sigma-Aldrich), N-(3-dimethylaminopropyl)-N'-ethylcarbodiimide hydrochloride (EDC, \geq 98%, Sigma-Aldrich) and phosphate buffered saline (PBS, Sigma-Aldrich) were used as received without purification. The StabilCoat® Immunoassay Stabilizer, Rb-IgG and anti-rabbit IgG produced in rabbits were purchased from Sigma-Aldrich. The vortex mixer was a TopMix FB15024

(Fisher Scientific). The dialysis tubing was Spectra/Por Dialysis membrane with a MWCO of 12000-14000 (Spectrum Laboratories). The silver coated colloidosomes and polymer shell colloidosomes were synthesized following a previous paper [20]. Briefly, Poly (methyl methacrylate-co-butyl acrylate) latex particles were synthesized via emulsion polymerization. The diameter of the latex particles was determined as 153 nm by dynamic light scattering using a Brookhaven Zeta-PALS. 2 mL of 5.6 wt% latex particles and 15 wt% L-Ascorbic acid suspension was added into a mixture of 4 mL Span 80 and 200 mL sunflower oil using a Silverson high shear mixer. Then the whole mixture was heated at 50 °C for 1 h, and then was centrifuged to get L-Ascorbic acid solution core capsules. Silver coated colloidosomes can then be prepared by using silver nitrate (AgNO_3) in the wash solution. The diameter of the water core is from 0.7 μm to 2 μm . The thickness of the polymer shells is the diameter of the latex, about 153 nm. .

Attachment of Rb-IgG to silver shell colloidosomes. A known mass of silver coated colloidosomes were dispersed in 0.5 wt% 4,4'-dithiodibutyric acid (DDA) solution using the vortex. The mixture was then gently mixed by a magnetic stirrer for 48 hours at room temperature. After the reaction, the whole mixture was centrifuged at 1500 rpm for 2 min. The supernatant was removed using a pipette. The modified silver shell capsules were washed and redispersed five times using ultra-pure water. 1 ml of modified silver coated colloidosomes was transferred to an eppendorf tube. 10 μl of N-hydroxysulfosuccinimide sodium salt (sulfo-NHS, 50 mg/ml) and 10 μl of N-(3-dimethylaminopropyl)-N'-ethylcarbodiimide hydrochloride (EDC, 50 mg/ml) were added to the eppendorf tube to activate the carboxylic acid of DDA on the modified silver shell surface. Then the eppendorf tube was put on a rotator for 20 min. After rotating, the suspension was centrifuged at 2000 rpm for 2 min at 25°C. The supernatant was removed via pipetting and the sediment was redispersed in PBS buffer solution using a vortex mixer. This washing process was repeated three times. After washing, 16.2 μl of Rb-IgG (12.35 mg/ml, rabbit antigen) was added into the colloidosome

suspension such that the concentration of Rb-IgG in the suspension was 200 $\mu\text{g/ml}$. The whole mixture was incubated with rotational mixing at 4°C for 1 h and washed three times using PBS buffer solution. The silver shell colloidosome protein attachment is achieved through peptide coupling which involves the activated carboxylic acid and the N-terminal of the protein. The modified silver coated colloidosomes were then stored at room temperature.

SPR gold film crosslinking. A glass slide coated with a gold film of 50 nm thickness was washed with 70% ethanol and dried with nitrogen gas. 500 μl of DDA in water (1 mM) was introduced to the central part of the gold film and rested for 1 h. 10 μl of sulfo-NHS (50 mg/ml) and 10 μl of EDC (50 mg/ml) were added to the DDA solution in the central part of the gold film and left for 30 min. After resting, the gold film was washed with ultra-pure water and dried with nitrogen gas. This washing was repeated three times. Then 500 μl anti-rabbit IgG (200 $\mu\text{g/ml}$) was placed and confined to the central area of the gold film and left for 1 h at 4°C . After resting, the gold film was washed with ultra-pure water and dried with nitrogen gas three times and stored in PBS solution at 4°C .

Targeting model - Immunoassay targeting. A home-built spectral Surface Plasmon Resonance biosensor setup was used to perform the immunoassay experiments ^[41]. Before the measurements, the silver shell colloidosomes were coated with rabbit Immunoglobulin G (IgG). In addition, the SPR gold film was immobilized with anti-rabbit IgG. The method for attaching this capture ligand is similar to the immobilization technique used for silver shell colloidosomes. Figure 1 shows the SPR experimental flow chart. Firstly, a known volume of the PBS solution was flowed into the cell for 10 min. After washing, the first data was recorded. Then a suspension of modified silver coated colloidosomes with rabbit antigen in PBS solution, was injected using a syringe. After the SPR channel was filled with solution, the second data was recorded. Then the cell was rotated by 90° and kept in this horizontal position for 10 min to allow the silver shell capsules to settle onto the gold film. This also allows sufficient time for the binding between the antigen crosslinked with the silver shell and

the antibody crosslinked with the gold film of SPR. After resting for 10 min, the third data was recorded and the cell was then rotated back to the vertical configuration. Finally, PBS solution was flowed into the cell for 10 min to wash away any unbound analyte. After washing, the fourth data was recorded. The reflectance spectrum is analyzed and the peak wavelength is recorded.

Dye encapsulation. To encapsulate dye in the silver shell colloidosomes, a mixture, which contained 5.6 wt% latex particle, 15 wt% L-Ascorbic acid and 2 wt% Allura Red, was prepared. 2 mL of this mixture was then added into a mixture of 200 mL sunflower oil and 4 mL Span 80 for emulsifying and sintering. After sintering, the sunflower oil was removed and the microcapsules with L-Ascorbic acid and Allura Red were redispersed in AgNO₃ solution to form a silver shell, sealing the capsules. All the other colloidosome preparation steps are the same as reported previously^[20].

Release by ultrasonic treatment. The ultrasonic treatment was performed by using an ultrasonic processor GEX 750 (Sonics & Materials Inc., USA) operating at 20 kHz and 50 W. The probe of the ultrasonicator was injected into a capsule suspension in a plastic tube. An ice bath was applied to ensure that the temperature change of the capsule suspension was less than 5 °C.

Sample characterization. The colloidosomes were imaged by scanning electron microscopy (SEM). A Zeiss X-beam FIB SEM was used at an accelerating voltage of 5.0 kV. A drop of particle suspension was air-dried on a stainless steel SEM stub overnight. The silver coated colloidosome samples were imaged without any treatment.

The silver shell colloidosomes were also imaged by transmission electron microscopy (TEM). An FEI Philips Tecnai 20 TEM was used at 200 keV (Tungsten, LB6) high-energy electron beam. A drop of colloidosome sample was added onto a TEM disc and then transferred to the specimen holder.

A Renishaw inVia Raman microscope equipped with two lasers (514.5 nm and 633 nm), microscope, video camera, X-Y-Z stage controller, and a 1200-groove grating was used for analyzing the structure of modified silver shell colloidosomes. The Ramascope-1000 system is a fully automatic Raman microscope.

The surface charge of silver coated colloidosomes was measured in aqueous suspensions at 20 °C using a Brookhaven ZetaPALS. The pH of the suspension was adjusted using buffer solution.

A UV-vis spectrophotometer equipped with a tungsten lamp (Thermo Scientific, model Helios Gamma) was used for spectrometry measurements. The dyed samples were characterized by spectrophotometry in 10 mm path length polystyrene cuvettes. The absorbance value at 500 nm was recorded using ultra-pure water as the reference.

The Thermo Scientific NanoDrop ND-1000 spectrophotometer was used to measure the concentration of protein samples without dilution. The module displays the UV spectrum, measured the protein's absorbance at 280 nm and calculated the concentration (mg/ml). Confocal laser scanning microscopy (CLSM) images were captured with a Leica TS confocal scanning system (Leica, Germany) equipped with a 63×/1.4 oil immersion objective.

RESULTS AND DISCUSSION

Modification of silver coated colloidosomes. Figure 2 shows the SEM, processed TEM images of the silver coated colloidosomes as well as the Raman spectra for non-modified and modified silver coated colloidosomes. The polymer shell colloidosomes are fully covered by lamellar silver particles and the diameter of the water core is around one to two microns. It can be seen that the modified silver coated colloidosomes have an additional peak at 223 cm^{-1} Raman shift. This is likely to correspond to a Ag-S bond^[42], and it indicates the successful modification reaction between the silver shell colloidosomes and 4, 4'-dithiodibutyric acid as shown schematically in Figure 3. Table 1 shows the Zeta potential of non-modified and

modified silver coated colloidosomes. When the pH reached 10, the Zeta potential of the non-modified colloidosomes was -63.2 ± 4.0 mV. One reasonable explanation is that during the synthesis some SDS surfactant attached onto the silver surface and caused the negative charge. Even after washing, a small amount of SDS remains^[43]. After modification, the silver coated colloidosomes became less negatively charged (-25.4 ± 4.1 mV). The increased Zeta potential could be because of the thiol chemistry replacing part of the silver surface of the colloidosomes. In addition, we used an excess of ascorbic acid and there may be trace amounts still in the capsules even after washing a few times. The Raman and electrophoresis results suggest successful modification of the colloidosomes surface. The modified silver coated colloidosomes were then used for Rb-IgG crosslinking and immunoassay experiments.

Targeting model - Immunoassay targeting. Figure 4 shows SPR reflectivity graphs of the antigen solution, non-modified silver shell colloidosomes and modified silver shell colloidosomes. Figure 5 shows a bar chart of the SPR wavelength shift after 10 min settling and after washing. The resonance wavelength exhibits as the dip in the distribution demonstrating sensitivity to antigen and silver shell colloidosomes deposition. Before measuring the reflectivity of modified samples, two blank tests were carried out to measure the quantitative red shift of the blank immunoassay reaction and to investigate if any physical adsorption exists between the silver coated colloidosomes and the gold surface of SPR. Two blank tests were: (i) antigen solution and (ii) non-modified silver shell colloidosomes. Figures 4a and 4b illustrate that when injecting antigen solution, there was a 2.3 nm red shift even after washing. This was caused by the attachment of antigens, which were paired with the antibodies on the gold surface of SPR. Figures 4c and 4d suggest that when injecting the non-modified silver shell colloidosomes, there was a 1.5 nm red shift at the '10 min' position. However, after washing, the reflectivity graph came back to the original position and there was almost no red shift. It can be seen from Figure 5 that the wavelength shift of non-modified samples was about negligible. This indicates that there is no obvious physical

adsorption between the silver coated colloidosomes and the gold surface. The red shift after 10 min of deposition can be simply explained by the settling of the colloidosomes onto the gold surface and they are easily washed away by the buffer solution. Figures 4e and 4f show SPR reflectivity graphs of modified silver shell colloidosomes. It is seen that there was a 2.1 nm red shift after washing. The red shift was caused by the binding between the antigen crosslinked with the silver shell and the antibody crosslinked with the gold film of SPR. After the immunoassay experiments for the modified silver shell colloidosomes, we removed the gold film and washed it a further three times. There were still many modified capsules on the gold film as shown in Figure 6. Figure 6a is a low magnification for the gold film. Figure 6b and c are different areas and different magnification of the film. For the gold substrate, which was reacted to unmodified silver shell colloidosomes, there was only a few impurities and dust on the surface, with no silver shells.

The silver shell colloidosomes for this experiment were modified by DDA solution and then attached to rabbit antigen. We used non-modified silver shell colloidosomes as a control experiment to see the attachment efficiency. The concentration of the antigen solution was measured using Nanodrop a ND-1000 Spectrometer. After the crosslinking reaction, the average supernatant concentration for non-modified and modified samples were tested to calculate the loading efficiency. The loading efficiency of non-modified silver shell colloidosomes is about 5.5 $\mu\text{g}/\text{mg}$ and 7.4 $\mu\text{g}/\text{mg}$ for modified silver shell colloidosomes. One reasonable explanation is that the silver shell can adsorb some antigens by physical adsorption [44, 45]. For modified samples, there existed both physical adsorption and chemical reactions. The modified silver shell colloidosome protein attachment is achieved through peptide coupling which involves the activated carboxylic acid and the N-terminal of the antigen protein. This chemical reactions can be demonstrated by the immunoassay SPR results. These two factors caused the lower antigen concentration of the supernatant.

Dye encapsulation. Figure 7 shows the release of Allura Red dye from colloidosomes.

The reason why we used Allura Red AC is that this dye will not affect the colloidosomes making process. It is small enough to diffuse from the porous polymer shells and is not too pH sensitive. The two samples were either sealed with a silver or polymer shell. Before measuring the dye release of silver coated colloidosomes, some blank tests were carried out to investigate if any chemical reactions exist between Allura Red dye, free-moving latex particles and silver particles. Three blank tests were: (1) Allura Red dye (28 mg) in ultra-pure water (20 mL); (2) Allura Red dye (28 mg) in ultra-pure water (18.6 mL) and latex particles (1.4 mL, 5.6 wt % particle suspension in ultra-pure water), which was stirred for 1 min; (3) Allura Red dye (28 mg) in ultra-pure water (18.6 mL), latex particles (1.4 mL, 5.6 wt % particle suspension in ultra-pure water) and 0.26 g silver particles, which were produced by mixing L-Ascorbic acid and AgNO_3 directly. The amount of silver in the control is the same as the colloidosomes. The release data was normalized by the amount of encapsulated dye. This is the amount of dye added to the experiment minus the amount measured in the waste oil and wash solution. All mixtures were transferred into 10 cm of dialysis tubing and immersed in gently stirred ultra-pure water (450 mL).

Figure 7 illustrates the dye release profiles for the blank tests. It can be observed that all three control samples (samples 1, 2 and 3) leaked without any trigger and have similar trends. The final release percentage of samples 2 and 3 was approximately 92%. For sample 1, the final release percentage was a little higher, around 96.5%. It should be noted that the free-moving latex can absorb a small amount of dye. Figure 7 also illustrates the dye release profile for polymer shell colloidosomes (sample 4). The release rate from polymer shell colloidosomes was slower than unencapsulated material in dialysis tubing and the time to reach 50 % release was approximately 210 h. This is slower than previously reported for fluorescein release and may be due to either the size of Allura red AC or an interaction with the latex. The final release percentage of sample 4 was approximately 78%. This is lower than the control samples and indicates that some dye was lost during the manufacturing process

and also possibly absorbed onto the latex particles.

The silver shell colloidosomes for this experiment were prepared by using 15 wt% L-ascorbic acid in the core and 0.1 wt% AgNO₃ in the wash solution at room temperature for 1 h. It can be seen that there was negligible dye outside the silver shell colloidosomes (sample 5) even after 400 h. When 5mL 1 wt% nitric acid was added to dissolve the silver shell (sample 6) at 65 °C for 10 min, the release occurred up to a maximum release yield of around 20 %. During the process of dissolving the silver shell, the high temperature (65 °C) and nitric acid may destroy some of the dye, which could account for the relatively low apparent encapsulation efficiency. The results of samples 5 and 6 indicate that the silver shell can totally seal the encapsulated material and that release from the silver shell can be triggered by dissolution of the shell upon addition of nitric acid.

Release by ultrasonic treatment. A suspension of microcapsules was subjected to ultrasound sonication at 20 kHz for different durations. Figure 8 shows SEM images of silver shell colloidosomes after various sonication times. It can be seen that some of the capsules were broken into fragments after 120 s of treatment and most of the capsules were destroyed after 240 s. Figure 9 shows CLSM images of dyed silver shell colloidosomes after various sonication times. The colloidosomes were dyed using Allura Red AC. It was seen that intact dyed silver shell colloidosomes were found without sonication. After 60 s and to more extent after 120 s of ultrasound treatment, the colloidosomes look broken, as supported by SEM images in figure 8. For longer times of ultrasound treatment (120 and 240 s), a significant number of the capsules were broken into fragments but still appear stained due to dye attached to capsule debris. After 240 s sonication, only a few colloidosomes remained intact. In the confocal images there are many small fluorescent pieces of capsule debris and there is an increase in background fluorescence indicating released dye.

For the ultrasound treatment with a high power of 50 W, a few minutes is enough to break the silver coated colloidosomes and release the dye solution. However, with lower

ultrasound intensities a relatively long duration time is needed to damage the silver coated colloidosomes ^[46]. Further studies using low power ultrasound will investigate this. The breakage of the capsules with ultrasound seems to be size dependent, however, the SEM images were not plentiful enough to quantify this. Another factor is the distance of the capsules from the ultrasound probe, with those nearer the probe, more likely to be broken.

Microscale silver shell colloidosomes should not be very toxic to cells, but after ultrasound treatment the nanoscale pieces of broken silver shells and silver ions may be toxic to biological systems ^[47, 48]. For future work, cell viability will be tested for silver shell samples with and without ultrasound treatment.

Targeted carriers for dye solution. The home-built flow cell channel was used to perform targeted carriers experiments. Figure 10 shows the experimental flow chart. A gold film, which was immobilized with anti-rabbit IgG, was set up at the bottom of the channel. Firstly, a known volume of the PBS solution was flowed into the channel. After washing, a suspension of dyed modified silver coated colloidosomes crosslinked with Rb-IgG in PBS solution, was injected using a syringe. After the channel was filled with the suspension, it was kept in this position for 10 min to allow the silver shell capsules to settle onto the gold film. After resting for 10 min, the PBS solution was flowed into the channel to wash away any unbound analyte. Finally, the gold film coating with dyed silver shell colloidosomes was subjected to ultrasound to break the shell and release the dye.

Figure 11 shows SEM images of the gold film after crosslinking with dyed silver shell colloidosomes. One can observe a large number of dyed silver coated colloidosomes attached on the gold film after the crosslinking reaction. The square crystals on the gold film are likely to be salt separating out from the buffer solution. This high efficiency of attachment illustrates the strong possibility for silver coated colloidosomes to be used as targeted carriers. Figure 12 shows SEM images of the gold film coated with dyed silver shell colloidosomes after ultrasound treatment. It can be seen that after 240 s of the capsules attached on the gold film

were destroyed into fragments with only very few capsules remaining intact. This indicates that the silver shell colloidosomes are promising to be used as targeted carriers for small molecules which can be released by ultrasound.

CONCLUSIONS

Our study has shown a novel type of silver coated colloidosomes which are capable for immunoassay targeting, small molecule encapsulation and triggered release by ultrasound. The colloidosomes were successfully demonstrated to encapsulate small molecules Allura Red AC and the shell of these structures was ruptured using ultrasound treatment. The colloidosomes were modified using 4,4'-dithiodibutyric acid and crosslinked with rabbit antigen. The Surface Plasmon Resonance which was used for an immunoassay sensitivity measurement proved that the functional colloidosomes crosslinking with the IgG can be captured by the anti-rabbit IgG immobilized on surface. The functional silver coated colloidosomes is believed to be promising for many future medical applications including targeted carriers for small bioactive molecules with controlled drug delivery and externally triggered release.

ASSOCIATED CONTENT

SUPPORTING INFORMATION

The Supporting Information is available free of charge on the ACS Publications website. Schematic diagram of home-built spectral Surface Plasmon Resonance (SPR).

AUTHOR INFORMATION

* Corresponding Author

Dr. Alexander F. Routh

E-mail address: afr10@cam.ac.uk

Tel: 01223765718; Fax: 01223765701

Department of Chemical Engineering and Biotechnology, University of Cambridge,
Pembroke Street, CB2 3RA, Cambridge, United Kingdom

ACKNOWLEDGMENT

The authors thank Dr Krzysztof Koziol (Department of Materials Science and Metallurgy, University of Cambridge) for his assistance with use of the Raman Spectroscope. The authors also thank Dr Richard Langford (Department of Physics, University of Cambridge) for his assistance with use of the scanning electron microscopy and the transmission electron microscopy. Many thanks for Dr Stuart Clarke (Department of Chemistry, University of Cambridge) for his advice about the modification reaction. Qian Sun, Ziyang Zhao and Hui Gao are grateful to the China Scholarship Council for funding. Yao Du is grateful to the Agency for Science Technology and Research (A*STAR) Singapore for funding.

REFERENCES

- [1] Kidane, A.; Bhatt, P. P. Recent Advances in Small Molecule Drug Delivery. *Curr. Opin. Chem. Biol.* **2005**, 9(4), 347-351.
- [2] Song, W.; He, Q.; Möhwald, H.; Yang, Y.; Li, J. B. Smart Polyelectrolyte Microcapsules as Carriers for Water-Soluble Small Molecular Drug. *J. Controlled Release* **2009**, 139(2), 160-166.
- [3] Eloy, J. O.; de Souza, M. C.; Petrilli, R.; Barcellosa, J. P. A.; Leeb, R. J.; Marchettia, J. M. Liposomes as Carriers of Hydrophilic Small Molecule Drugs: Strategies to Enhance Encapsulation and Delivery. *Colloids Surf. B: Biointerfaces* **2014**, 123, 345-363.
- [4] Gao, H.; Goriacheva, O. A.; Tarakina, N. V.; Sukhorukov, G. B. Intracellularly

- Biodegradable Polyelectrolyte/Silica Composite Microcapsules as Carriers for Small Molecules. *ACS Appl. Mat. Interfaces* **2016**, 8(15), 9651-9661.
- [5] Vrignaud, S.; Benoit, J. P.; Saulnier, P. Strategies for the Nanoencapsulation of Hydrophilic Molecules in Polymer-Based Nanoparticles. *Biomaterials* **2011**, 32(33), 8593-8604.
- [6] Kim, C. S.; Mout, R.; Zhao, Y.; Yeh, Y. C.; Tang, R.; Jeong, Y.; Duncan, B.; Hardy, J. A.; Rotello, V. M. R. Co-Delivery of Protein and Small Molecule Therapeutics Using Nanoparticle-Stabilized Nanocapsules. *Bioconjug Chem.* **2015**, 26(5), 950-954.
- [7] Torchilin, V. P. Recent Advances with Liposomes as Pharmaceutical Carriers. *Nat Rev Drug Discov.* **2005**, 4(2): 145-160.
- [8] Velev, O. D.; Furusawa, K.; Nagayama, K. Assembly of Latex Particles by Using Emulsion Droplets as Templates. 1. Microstructured Hollow Spheres. *Langmuir* **1996**, 12(10): 2374-2384.
- [9] Lensen, D.; Vriezema, D. M.; Van Hest, J. Polymeric Microcapsules for Synthetic Applications. *Macromol. Bioscience* **2008**, 8(11): 991-1005.
- [10] Yow, H. N.; Routh, A. F. Formation of Liquid Core-Polymer Shell Microcapsules. *Soft Matter* **2006**, 2(11), 940-949.
- [11] Frost & Sullivan, Microencapsulation Raises Profile of Pesticides, in Laboratory Talk, Pro-Talk Ltd, Letchworth, **2002**. Available from: <http://www.laboratorytalk.com/news/fro/fro119.html>.
- [12] Pavlov, A. M.; Sapelkin, A. V.; Huang, X.; P'ng, K. M. Y.; Bushby, A. J.; Sukhorukov, G. B.; Skirtach, A. G. Neuron Cells Uptake of Polymeric Microcapsules and Subsequent Intracellular Release. *Macromol. Bioscience* **2011**, 11(6), 848-854.
- [13] Dinsmore, A. D.; Hsu, M. F.; Nikolaidis, M. G.; Marquez, M.; Bausch, A. R.; Weitz, D. A. Colloidosomes: Selectively Permeable Capsules Composed of Colloidal Particles. *Science* **2002**, 298(5595), 1006-1009.

- [14] Kim, E.; Kim, D.; Jung, H.; Lee, J.; Paul, S.; Selvapalam, N.; Yang, Y.; Lim, N.; Park, C. G.; Kim, K. Facile, Template-Free Synthesis of Stimuli-Responsive Polymer Nanocapsules for Targeted Drug Delivery. *Angew. Chem.* **2010**, 122(26), 4507-4510.
- [15] Kozlovskaya, V.; Kharlampieva, E.; Mansfield, M. L.; Sukhishvili, S. A. Poly (methacrylic acid) Hydrogel Films and Capsules: Response to pH and Ionic Strength, and Encapsulation of Macromolecules. *Chem. Mater.* **2006**, 18(2), 328-336.
- [16] Nomura, T.; Routh, A. F. A Novel Method of Fabrication of Latex-Stabilized Water-Core Colloidosomes at Room Temperature. *Langmuir* **2010**, 26(24), 18676-18680.
- [17] Gåserød, O.; Sannes, A.; Skjåk-Bræk, G. Microcapsules of Alginate-Chitosan. II. A Study of Capsule Stability and Permeability. *Biomaterials* **1999**, 20(8), 773-783.
- [18] Keen, P. H. R.; Slater, N. K. H.; Routh, A. F. Encapsulation of Amylase in Colloidosomes. *Langmuir* **2014**, 30(8), 1939-1948.
- [19] Yow, H. N.; Routh, A. F. Release Profiles of Encapsulated Actives from Colloidosomes Sintered for Various Durations. *Langmuir* **2008**, 25(1), 159-166.
- [20] Sun, Q.; Routh, A. F. Aqueous Core Colloidosomes with a Metal Shell. *Eur. Polym. J.* **2016**, 77: 155-163.
- [21] Dennis, S.; Sebastian, S. Monodispersity and Size Control in the Synthesis of 20-100 nm Quasi-Spherical Silver Nanoparticles by Citrate and Ascorbic Acid Reduction in Glycerol-Water Mixtures. *Chem. Commun.* **2012**, 48(69), 8682-8684.
- [22] Yukiyasu, K.; Mari, Y.; Masami, N. Facile Size-Regulated Synthesis of Silver Nanoparticles by Controlled Thermolysis of Silver Alkyl Carboxylates in the Presence of Alkyl Amines with Different Chain Lengths. *J. Colloid Interface Sci.* **2006**, 300(1), 169-175.
- [23] Sun, Y.; Xia, Y. Shape-Controlled Synthesis of Gold and Silver Nanoparticles. *Science* **2002**, 298(5601), 2176-2179.
- [24] Delehanty, J. B.; Boeneman, K.; Bradburne, C. E.; Robertson, K.; Bongard, J. E.;

- Medintz, I. L. Peptides for Specific Intracellular Delivery and Targeting of Nanoparticles: Implications for Developing Nanoparticle-Mediated Drug Delivery. *Therapeutic delivery* **2010**, 1(3), 411-433.
- [25] Seker, U. O. S.; Demir, H. V. Material Binding Peptides for Nanotechnology. *Molecules* **2011**, 16(2), 1426-1451.
- [26] Liong, M.; Lu, J.; Kovichich, M.; Xia, T.; Ruehm, S. G.; Nel, A. E.; Tamanoi, F.; Zink, J. I. Multifunctional Inorganic Nanoparticles for Imaging, Targeting, and Drug delivery. *ACS Nano* **2008**, 2(5), 889-896.
- [27] Langer, R.; Peppas, N. A. Advances in Biomaterials, Drug Delivery, and Bionanotechnology. *AIChE J.* **2003**, 49(12), 2990-3006.
- [28] Chae, M. Y.; Czarnik, A. W. Fluorometric Chemodosimetry Mercury (II) and Silver (I) Indication in Water via Enhanced Fluorescence Signaling. *J. Am. Chem. Soc.* **1992**, 114(24), 9704-9705.
- [29] Zhang, F.; Braun, G. B.; Shi, Y.; Zhang, Y.; Sun, X.; Reich, N. O.; Zhao, D.; Stucky, G. Fabrication of Ag@SiO₂@Y₂O₃: Er Nanostructures for Bioimaging: Tuning of the Upconversion Fluorescence with Silver Nanoparticles. *J. Am. Chem. Soc.* **2010**, 132(9), 2850-2851.
- [30] Zhang, J.; Fu, Y.; Chowdhury, M. H.; Lakowicz, J. R. Metal-Enhanced Single-Molecule Fluorescence on Silver Particle Monomer and Dimer: Coupling Effect between Metal Particles. *Nano lett.* **2007**, 7(7), 2101-2107.
- [31] Lakowicz, J. R.; Malicka, J.; D'Auria, S.; Gryczynski, I. Release of the Self-Quenching of Fluorescence near Silver Metallic Surfaces. *Anal. Biochem.* **2003**, 320(1), 13-20.
- [32] Bhagwat, A. A. Rapid Detection of Salmonella from Vegetable Rinse-Water Using Real-Time PCR. *Food Microbiol.* **2004**, 21(1), 73-78.
- [33] Giepmans, B. N. G.; Adams, S. R.; Ellisman, M. H.; Tsien, R. Y. The Fluorescent Toolbox for Assessing Protein Location and Function. *Science* **2006**, 312(5771), 217-224.

- [34] Yang, G. J.; Huang, J. L.; Meng, W. J.; Shen, M.; Jiao, X. A. A Reusable Capacitive Immunosensor for Detection of Salmonella Spp. Based on Grafted Ethylene Diamine and Self-Assembled Gold Nanoparticle Monolayers. *Anal. Chim. Acta* **2009**, 647(2), 159-166.
- [35] Zhang, D.; Yan, Y.; Li, Q.; Yu, T. X.; Cheng, W.; Wang, L.; Ju, H.; Ding, S. Label-Free and High-Sensitive Detection of Salmonella Using a Surface Plasmon Resonance DNA-Based Biosensor. *J. biotechnol.* **2012**, 160(3): 123-128.
- [36] Homola, J.; Yee, S. S.; Gauglitz, G. Surface Plasmon Resonance Sensors: Review. *Sens. actuators. B Chem.* **1999**, 54(1): 3-15.
- [37] Green, R. J.; Frazier, R. A.; Shakesheff, K. M.; Davies, M. C.; Roberts, C. J.; Tendler, S. J. Surface Plasmon Resonance Analysis of Dynamic Biological Interactions with Biomaterials. *Biomaterials* **2000**, 21(18), 1823-1835.
- [38] Stock, N.; Biswas, S. Synthesis of Metal-Organic Frameworks (MOFs): Routes to Various MOF Topologies, Morphologies, and Composites. *Chem. Rev.* **2011**, 112(2), 933-969.
- [39] Shekhah, O.; Wang, H.; Kowarik, S.; Schreiber, F.; Paulus, M.; Tolan, M.; Sternemann, C.; Evers, F.; Zacher, D.; Fischer, R. A.; Wöll, C. Step-by-Step Route for the Synthesis of Metal-Organic Frameworks. *J. Am. Chem. Soc.* **2007**, 129(49), 15118-15119.
- [40] Shchukin, D. G.; Ustinovich, E. A.; Sukhorukov, G. B.; Möhwald, H.; Sviridov, D. V. Metallized Polyelectrolyte Microcapsules. *Adv. Mater.*, **2005**, 17(4), 468-472.
- [41] Hong, X.; Hall, E. A. H. Contribution of Gold Nanoparticles to the Signal Amplification in Surface Plasmon Resonance. *Analyst* **2012**, 137(20), 4712-4719.
- [42] Saikin, S. K.; Olivares-Amaya, R.; Rappoport, D.; Stopa, M.; Aspuru-Guzik, A. On the Chemical Bonding Effects in the Raman Response: Benzenethiol Adsorbed on Silver Clusters. *Phys. Chem. Chem. Phys.* **2009**, 11(41), 9401-9411.
- [43] Szczepanowicz, K.; Stefanska, J.; Socha, R. P.; Warszynski, P. Preparation of Silver Nanoparticles via Chemical Reduction and Their Antimicrobial Activity. *Physicochem.*

Probl. Miner. Process **2010**, 45, 85-98.

- [44] Butler, J. E.; Nessler, L. Ni R.; Joshi, K. S.; Suter, M.; Rosenberg, B.; Chang, J.; Brown, W.R.; Cantarero, L. A. The Physical and Functional Behavior of Capture Antibodies Adsorbed on Polystyrene. *J. Immunol. Methods* **1992**, 150(1-2), 77-90.
- [45] Henriksen-Lacey, M.; Christensen, D.; Bramwell, V. W.; Lindenstrøm, T.; Agger, E. M.; Andersen, P.; Perrie, Y. Liposomal Cationic Charge and Antigen Adsorption are Important Properties for The Efficient Deposition of Antigen at The Injection Site and Ability of The Vaccine to Induce a CMI Response. *J. Control. Release* **2010**, 145(2), 102-108.
- [46] Shchukin, D. G.; Gorin, D. A.; Möhwald, H. Ultrasonically Unduced Opening of Polyelectrolyte Microcontainers. *Langmuir* **2006**, 22(17), 7400-7404.
- [47] Zhou, H.; Mu, Q.; Gao, N.; Liu, A.; Xing, Y.; Gao, S.; Zhang, Q.; Qu, G.; Chen, Y.; Liu, G.; Zhang, B.; Yan, B. A Nano-combinatorial Library Strategy for The Discovery of Nanotubes with Reduced Protein-binding, Cytotoxicity, and Immune Response. *Nano Lett.* **2008**, 8(3), 859-865.
- [48] Mu, Q.; Jiang, G.; Chen, L.; Zhou, H.; Fourches, D.; Tropsha, A.; Yan, B. Chemical Basis of Interactions between Engineered Nanoparticles and Biological Systems. *Chem. Rev.* **2014**, 114(15), 7740-7781.

FIGURE CAPTION

Figure 1. SPR experimental flow chart.

Figure 2. SEM and processed TEM images of the silver coated colloidosomes: (a) SEM image of silver coated colloidosomes; (b) processed TEM image of a single silver coated colloidosome; and (c) Raman spectra for non-modified and modified silver coated colloidosomes.

Figure 3. Possible reaction between the silver surface and 4, 4'-dithiodibutyric acid (DDA).

Figure 4. SPR reflectivity graphs: (a) (b) antigen solution; (c) (d) non-modified silver shell colloidosomes; (e) (f) modified silver shell colloidosomes, b, d and f graphs are presented as magnified insets for clarity purpose to illustrate shifts in spectra.

Figure 5. Bar chart of the SPR wavelength shift for after 10 min settling and after washing.

Figure 6. SEM images of modified silver shell colloidosomes attached on gold film after washing.

Figure 7. Release of Allura Red dye from colloidosomes sealed with a silver shell, polymer shell and unsealed. Addition of nitric acid triggered the release from colloidosomes sealed with a silver shell. Error bars of the standard error of measurements, typically $\pm\sim 3\%$, are not shown for clarity.

Figure 8. SEM images of silver shell colloidosomes after various sonication times: (a) untreated; (b) 120 s and (c) 240 s.

Figure 9. CLSM images of dyed silver shell colloidosomes after various sonication times: (a) untreated; (b) 60 s; (c) 120 s and (d) 240 s.

Figure 10. Targeted carriers experimental flow chart.

Figure 11. SEM images of the gold film after crosslinking with dyed silver shell colloidosomes.

Figure 12. SEM images of different parts of the gold film coated with dyed silver shell colloidosomes after 240 s of ultrasound treatment.

Figure 1:

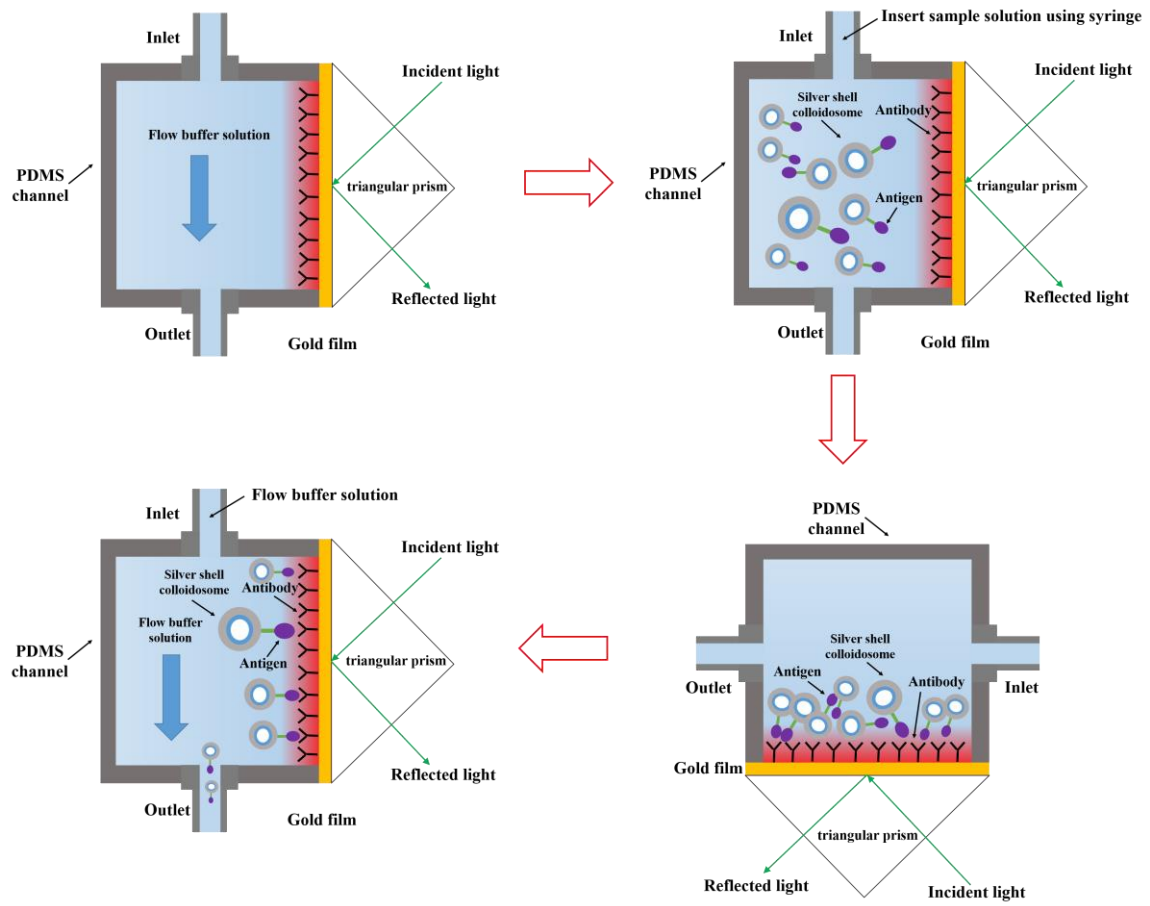


Figure 2:

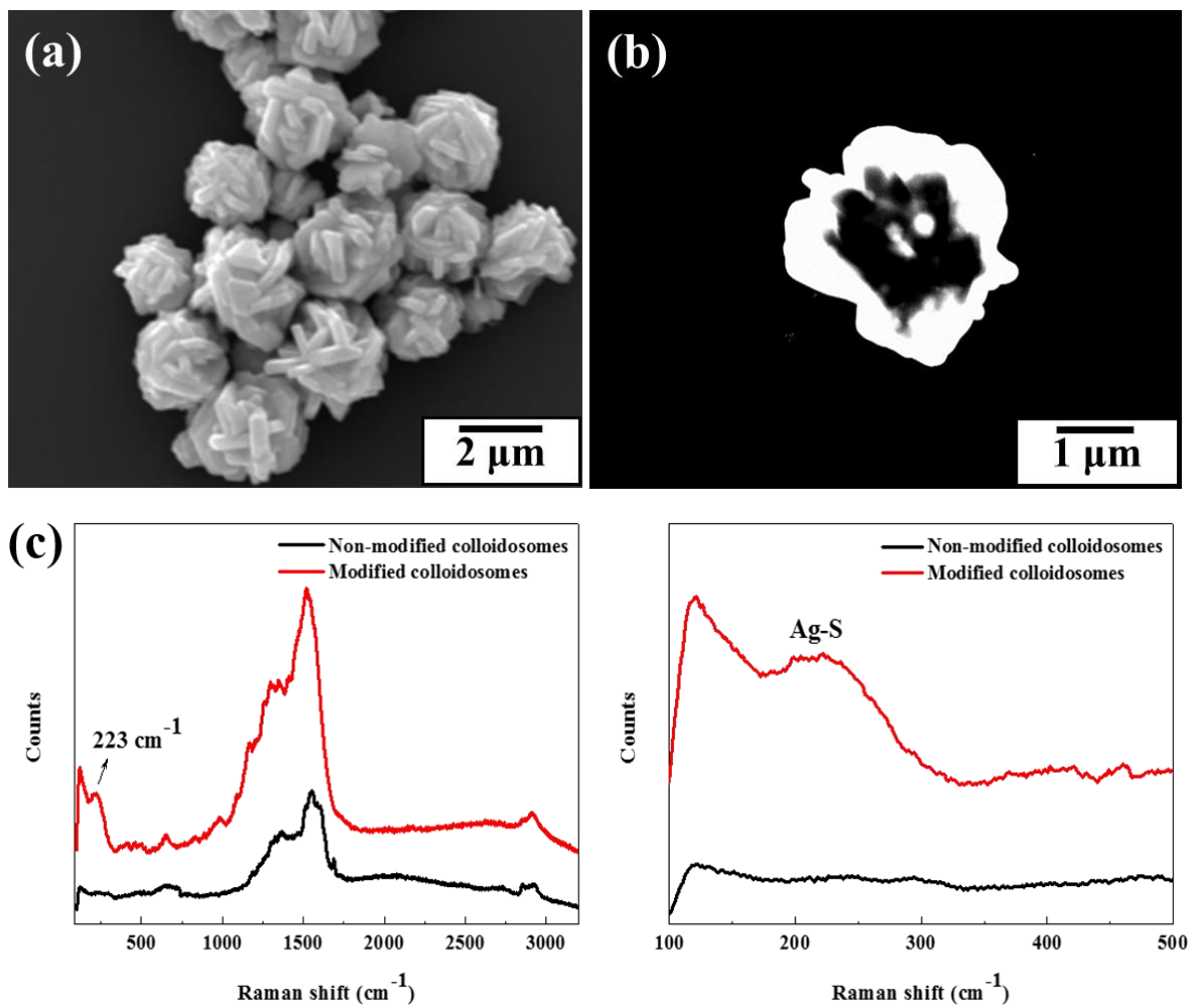


Figure 3:

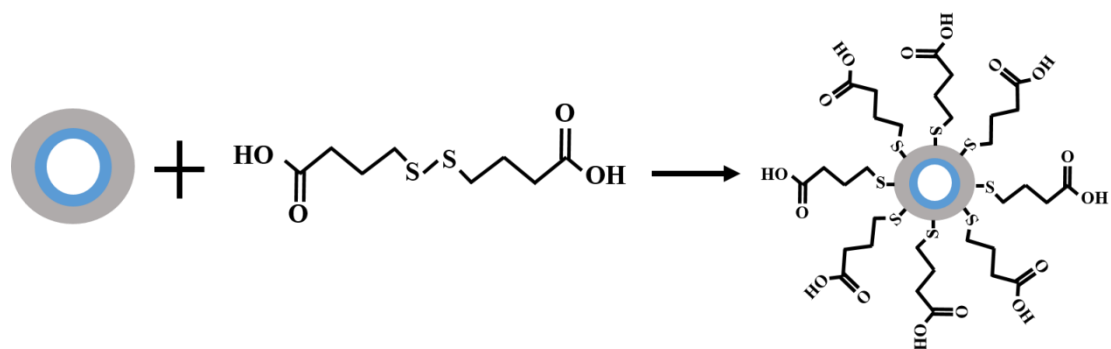


Figure 4:

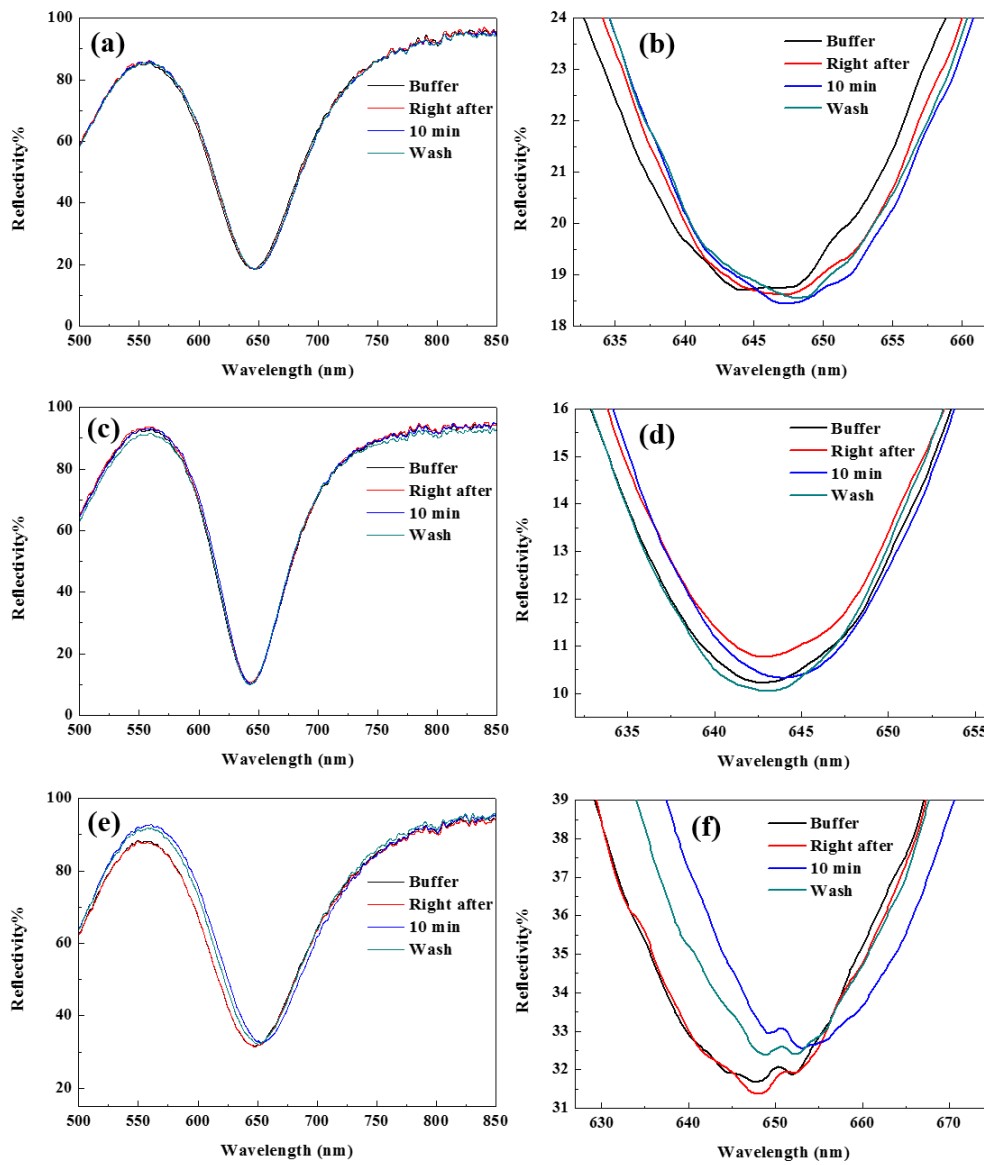


Figure 5:

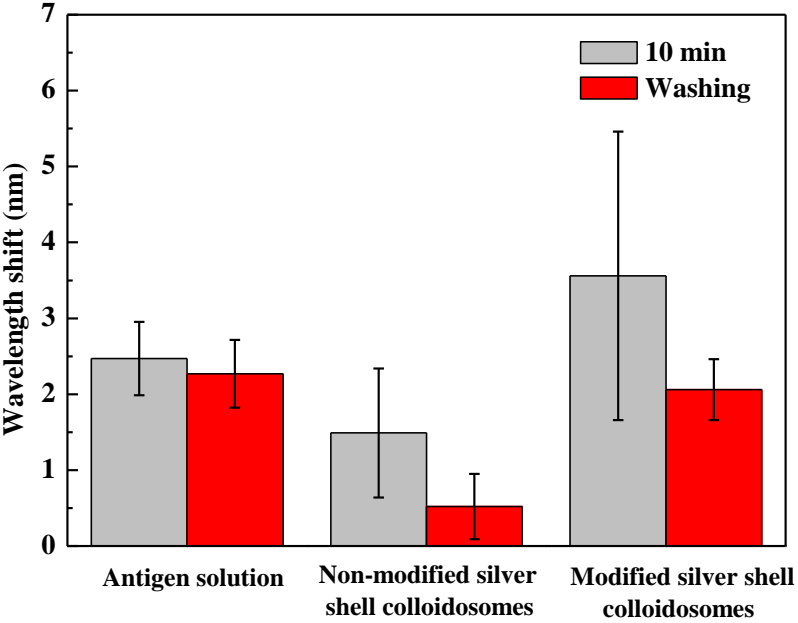


Figure 6:

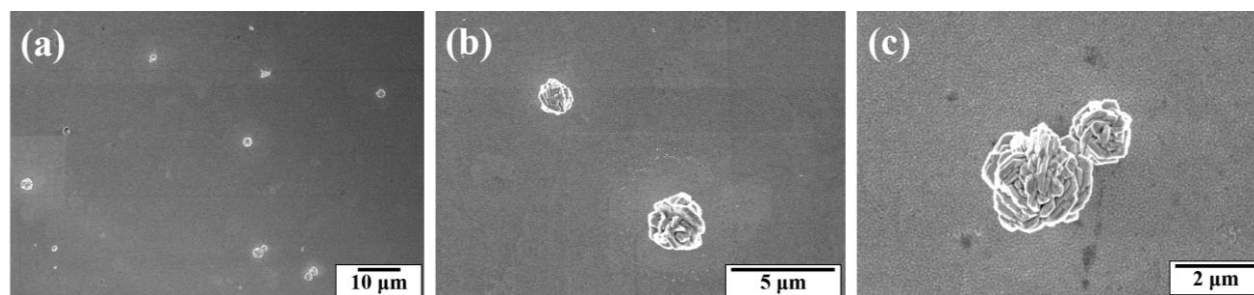


Figure 7:

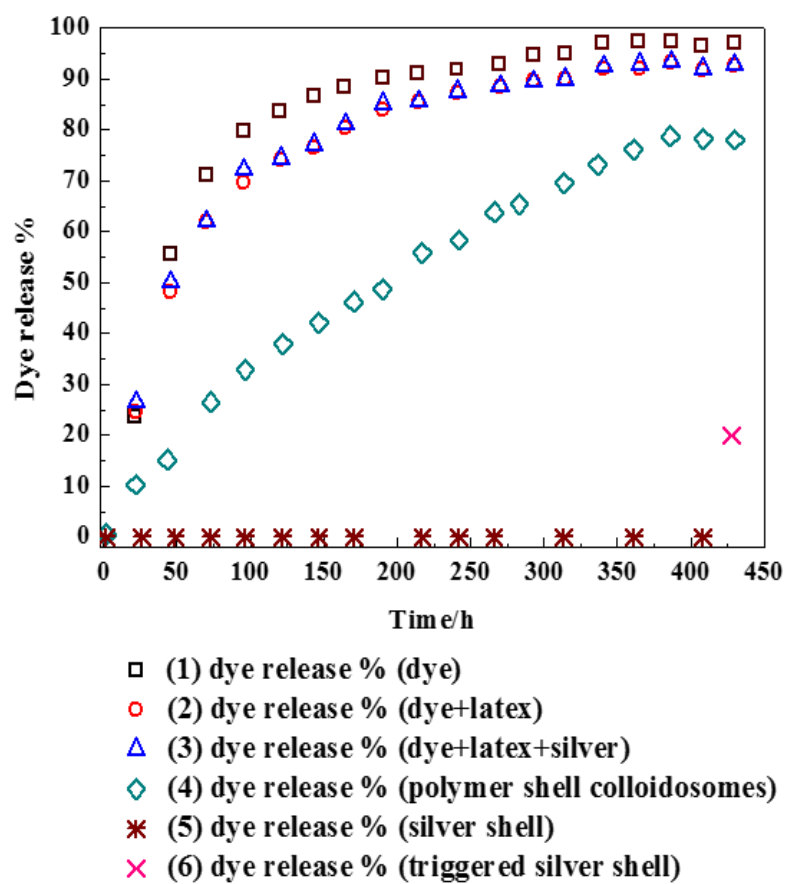


Figure 8:

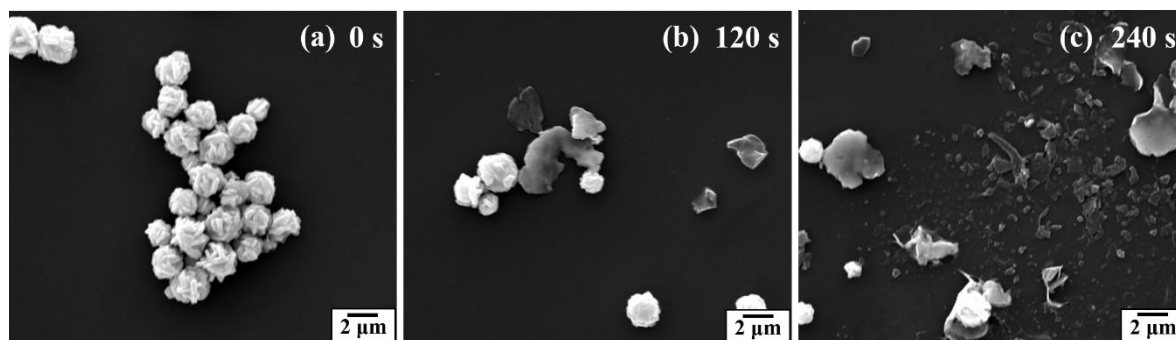


Figure 9:

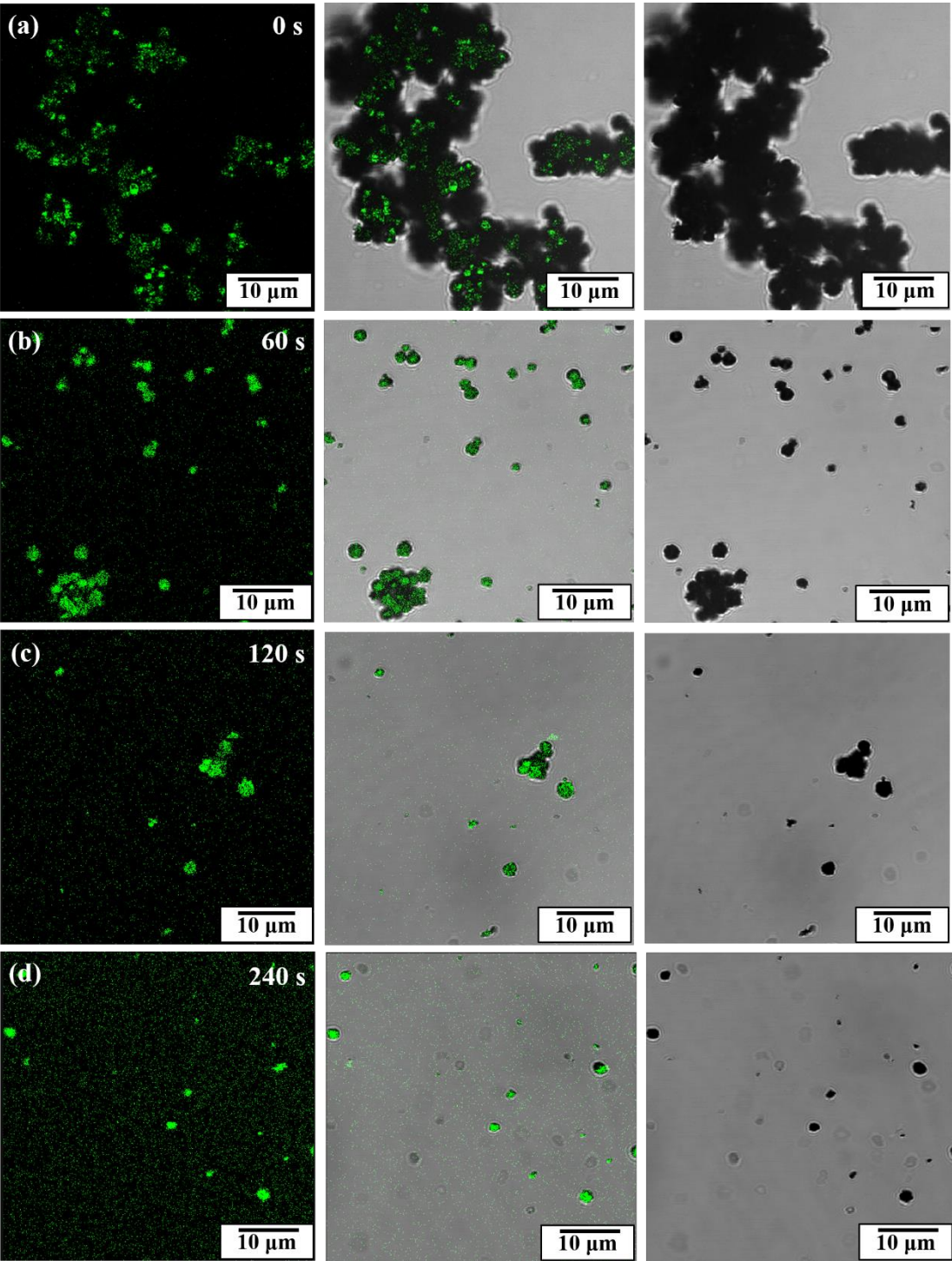


Figure 10:

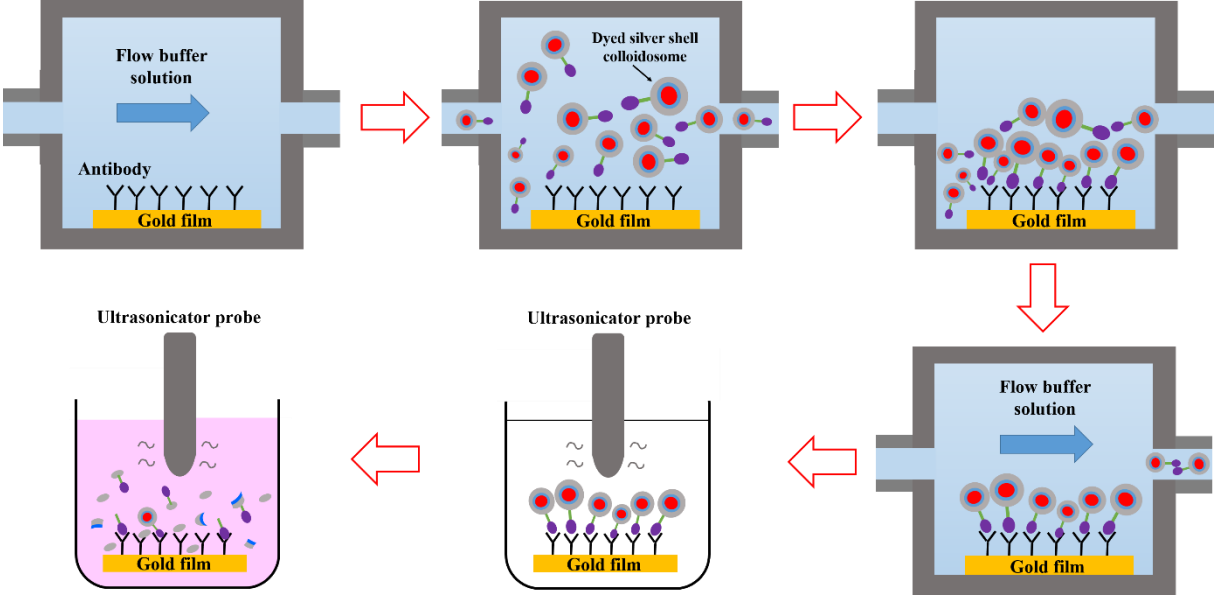


Figure 11:

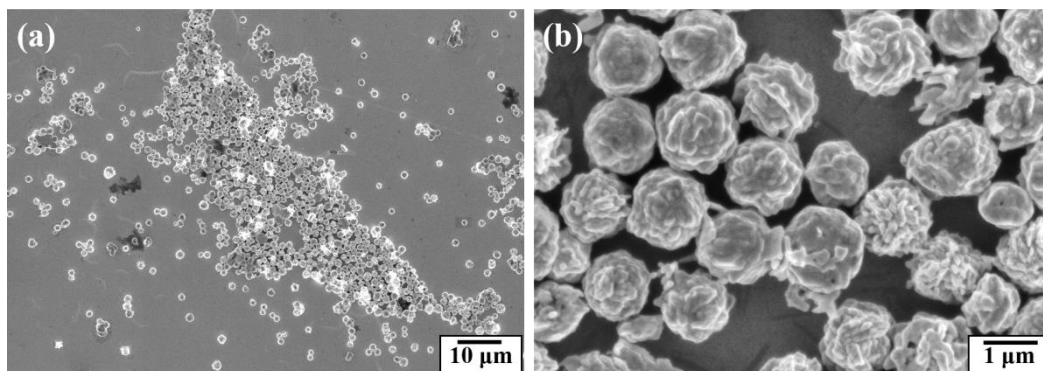


Figure 12:

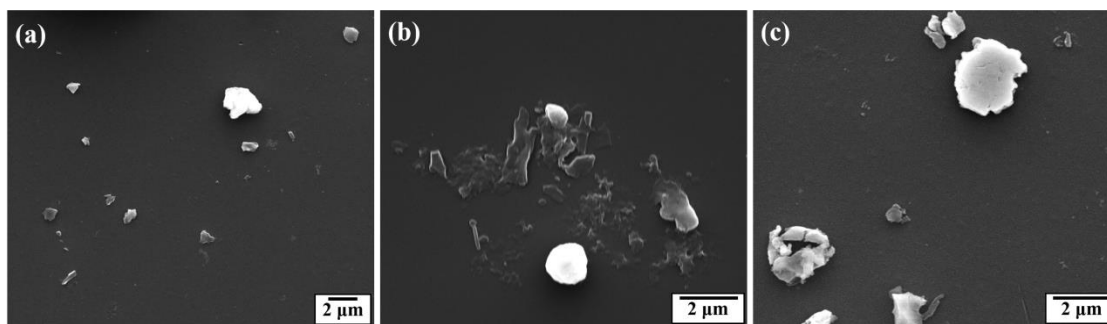
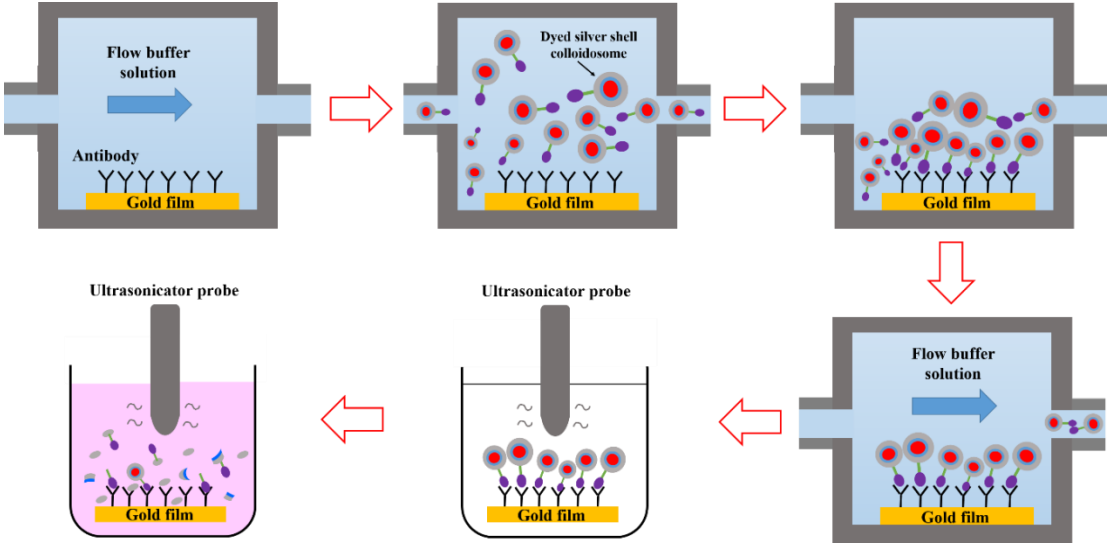


Table 1. Zeta potential of non-modified and modified silver coated colloidosomes

Sample	Zeta potential (mV)	
	pH = 7	pH = 10
Non-modified sample	- 53.9 ± 1.1	- 63.2 ± 4.0
Modified sample	- 46.2 ± 1.0	-25.4 ± 4.1

Table of contents entry



Impermeable aqueous core capsules are made bio-specific, using receptor proteins, and release is achieved using ultrasound